Optics & Laser Technology 138 (2021) 106920

Contents lists available at ScienceDirect

Optics and Laser Technology

journal homepage: www.elsevier.com/locate/optlastec

Full length article

Widely tunable 780 nm distributed feedback laser based on high-order surface isolation grooves

Xia Liu [a,b], Yongyi Chen [a,*], Yugang Zeng [a,*], Li Qin [a], Liang Lei [a], Peng Jia [a], Hao Wu [a], Dezheng Ma [a,b], Chunkao Ruan [a,b], Yongqiang Ning [a], Lijun Wang [a,c]

[a] State Key Laboratory of Luminescence and Applications, Changchun Institute of Optics, Fine Mechanics and Physics, Chinese Academy of Sciences, Changchun 130033, China
[b] Center of Materials Science and Optoelectronics Engineering, University of Chinese Academy of Sciences, Beijing 100049, China
[c] Peng Cheng Laboratory No.2, Xingke 1st Street, Nanshan, Shenzhen, China

ARTICLE INFO

Keywords:
Tunable DFB laser
laser diode

ABSTRACT

Widely tunable distributed feedback (DFB) lasers based on surface isolation grooves were developed using i-line lithography. Periodic p-electrodes on mesas enabled the realization of a great tunability. It is to be mentioned that, our device reached a wavelength tuning range of approximately 17.5 nm by only one pair of electrodes under both temperature and current variation with the help of order hop. A single longitudinal mode with continuous-wave output power reached up to 132.8 mW/facet for a drive current of 400 mA at 20 °C. The side-mode suppression ratio reached 36.25 dB. The wide tuning range and the simple fabrication steps promise our device an immense potential as light source in many applications such as atomic clocks and gas sensing.

1. Instruction

Tunable DFB laser diodes has many applications in optical communication systems, LiDAR, sensing, and so on [1–6]. The 780 nm tunalbe DFB laser is mainly used as light sources for pumping the Rb D2 transition, as used in Rb atomic clocks [7–10], magnetometers [11], precision gyroscopes [12], gas sensing [13], and LAN communication [14].

To the best of our knowledge, current laser diodes around 780 nm DFB lasers are mostly based on complicated nanoscale lithography or imprint and etching techniques [15,16,17]. This is making the device difficult to fabricate and expensive.

In our previous works, we had already proposed a regrowth-free method to fabricate gain coupled DFB laser diodes with isolation grooves and periodic p-electrodes to achieve single-longitudinal-mode (SLM) with a high side-mode suppression ratio (SMSR) [18,19]. In this paper, by properly designed the lasing wavelength and the period, we aim at fabricating 780 nm gain-coupled structure DFB laser and optimizing tuning range under the help of the order hop. By using only one pair of electrodes, our device reached a tuning rang of more than 17.5 nm, changing both the current (from 90 to 400 mA) and the temperature (from 10 to 45 °C). Our technique of achieving large tuning range without using secondary epitaxy or nano scale lithography has great potential for large scale production and will promote the applications in gas sensing and other many other fields.

2. Structure and fabrication

The chip of the device was prepared by metal–organic chemical vapor deposition (MOCVD). The active region of the device is composed of AlInGaAs/AlGaAs.

Fig. 1(a) provides a schematic diagram of the total structure. The electrodes are in the middle of the mesas. The multilayered structure of the chip is shown in Fig. 1(b), The active region is composed of a single quantum well and other gradient layers.Fig. 1(c) shows the structure of the surface mesas and isolation grooves. Currents are injected into the active region from the electrode windows. The lasing wavelength of the DFB laser depends on the period of surface grooves structure [20], and the width of one groove is 3 μm (L_g = 3 μm) in Fig. 1(c). The structure determines that the surface grooves structure acts as high order slot laser [21]. The surface isolation grooves can be seen under scanning electron microscope (SEM) in Fig. 1(d). Periodic electrical injections are formed, leading to the gain differences in the active region.

* Corresponding authors at: State Key Laboratory of Luminescence and Applications, Changchun Institute of Optics, Fine Mechanics and Physics, Chinese Academy of Sciences, Changchun 130033, China.
E-mail addresses: chenyy@ciomp.ac.cn (Y. Chen), zengyg@ciomp.ac.cn (Y. Zeng).

https://doi.org/10.1016/j.optlastec.2021.106920
Received 20 August 2020; Received in revised form 30 December 2020; Accepted 4 January 2021
Available online 25 January 2021

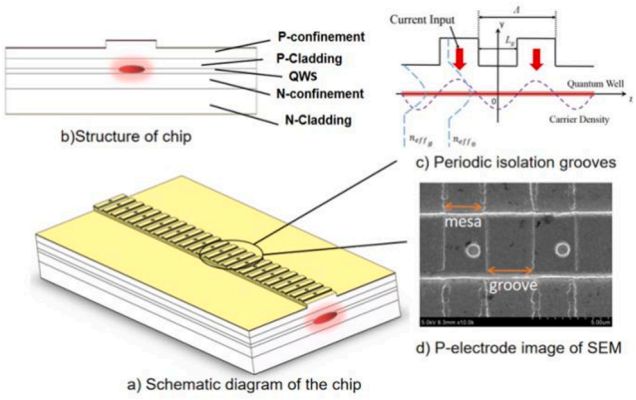

Fig. 1. Device schematic (a) schematic diagram of the chip, (b) structure of the epitaxy, (c) schematic diagram of the surface periodic isolation grooves, and (d) SEM image of the p-electrode.

First, we used photolithography (i-line) and inductively coupled plasma (ICP) etching to pattern the periodic isolation grooves with a period of 6.06 μm ($\Lambda = 6.06$ μm). Second, we patterned the 4 μm wide ridge waveguide of the device, again using i-line lithography and ICP etching. Third, we patterned the periodic electrode windows on the mesas of the unetched top of the isolation grooves on a new silica isolation layer, creating periodic current injection channels. Finally, 500 nm metal was deposited on the surface of the epitaxial wafer by magnetron sputtering. We cleaved the chips into 1 mm cavity length and coated one facet of the device to 95% anti-reflection (AR). The other facet of the device had a high-reflection (HR)-coating (95% power reflection assumed). The device was bonded p-side down on the heat sinks and placed on a thermoelectric cooler (TEC) controlled plate to maintain or tune the operating temperature.

According to our previous work [22],The periodic electrodes lead to a gain contrast in the quantum well resulting in a gain coupled mechanism.

3. Experiment results and discussion

A continuous-wave (CW) test was carried out based on the TEC at 20 °C. The power-voltage-current (P-I-V) characteristics and electro-optical efficiency of the device are shown in Fig. 2 (measured by Newport PMKIT-15-01). The PIV curve in Fig. 2 is obtained by emitting one facet of the device and the conversion efficiency is calculated by doubling the single facet's tested power. The device had a threshold current of 110 mA for a cavity length of 1 mm and ridge width of 4 μm. Single longitudinal mode operation reached up to 132.8 mW/facet at 400 mA. Obviously, the power increased linearly from 110 to 400 mA.

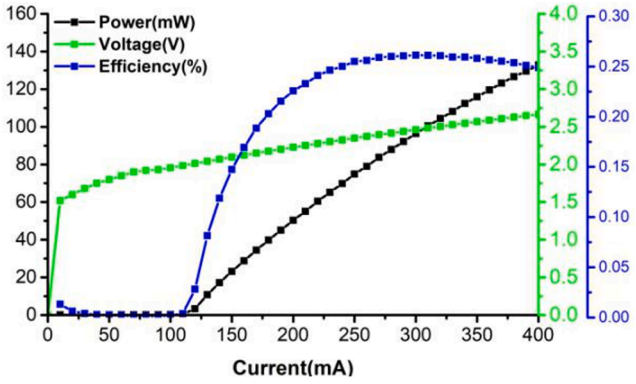

Fig. 2. CW power-voltage-current characteristics and electro-optical efficiency profiles at 20 °C.

The slope efficiency of one facet reached 0.28 W/A. Fig. 2 shows that the conversion efficiency increases rapidly in the range 110–250 mA. When the current reached 270 mA, the conversion efficiency was over 26%, because several electron-hole pairs are recombining when the current injection increases. It decreased slowly from 270 to 400 mA. Once the current exceeded 270 mA, the conversion efficiency decreased because of the accumulated thermal effect [23].

The spectra characteristics at different currents at 20 °C are clearly shown in Fig. 3.The spectra were measured directly by coupling the laser using a 10 μm core diameter fiber-linking YOKOGAWA AQ6370C optical spectrum analyzer. Fig. 3 shows that the wavelengths drift with the increase of current. Notice that, there is a order hop when the current exceeds 280 mA. It is due to the structure of high order surface isolation grooves. According to the formula: $M\lambda/2 = \Lambda N_{eff}$. Here, M is the lasing order,λ is the lasing wavelength. Λ is the period of the isolation grooves, which is 6 μm in our structure. N_{eff} is the effective index, which is about 3.447 calculated by COMSOL. At such a large period of 6 μm, different orders have different lasing wavelengths. By taking the advantage of order hop, the tuning range can be easily enlarged when changing the current and the temperature. As shown in Fig. 3, the tuning range can reach about 3 nm under 20 °C by changing the current only(from 90 to 400 mA), whose drift coefficient is much larger than surface grating DFB laser [24], 3 times larger than lateral grating DFB laser using nano-imprint lithography [17].

Fig. 4 shows the threshold of the device at different operating temperatures. The threshold increases with the temperature [25], which is due to the decrease of gain versus temperature. The lasing wavelengths of the device versus different operating temperatures and currents are shown in Fig. 5. The results show that the lasing wavelength mainly increase with temperature and current. We can see mode hops when tuning the current. It is because the device is AR/HR coated, which brings mode hop between different FP modes. The tuning spectrum in Fig. 5. is much alike a DBR laser [26],However, our device has a wider tuning range of 17.5 nm,5 times of 780 nm DBR laser [27]. The lasing wavelengths at the different temperatures overlap, which can cover a continuous wavelength. The expected tunable phenomenon is achieved. Given a current at 300 mA, as shown in Fig. 6, we see that the wavelength red-shifts. The SMSR are all over 30 dB during the temperature variation.

The tuning range of the device can be concluded from Fig. 7, Fig. 7 demonstrates that the working wavelength of the DFB laser device can be tuned from 775.5 to 793 nm under changing temperature and current injection. In this working range,the photoelectric conversion efficiency, disaster prevention, and tunable characteristics of the device are taken into account. Fig. 7. also shows a good SLM property with high SMSR

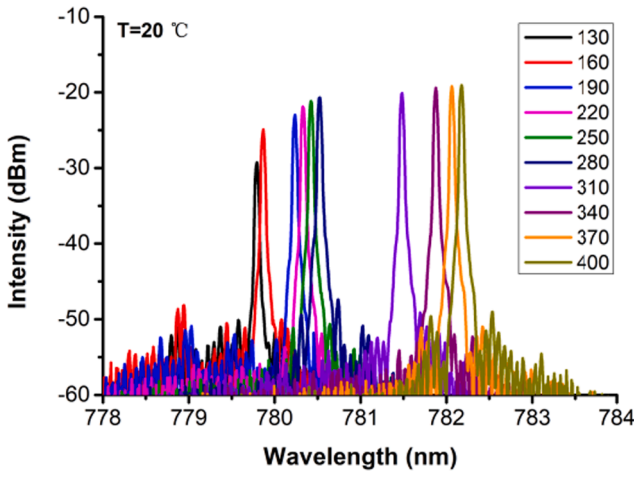

Fig. 3. CW spectrum characteristics of complex-coupled DFB laser for different injection currents at 20 °C.

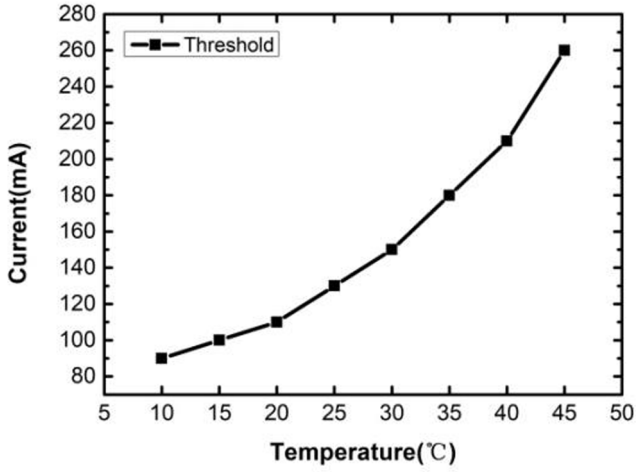

Fig. 4. Threshold of the DFB laser diode for temperatures from 10 to 45 °C.

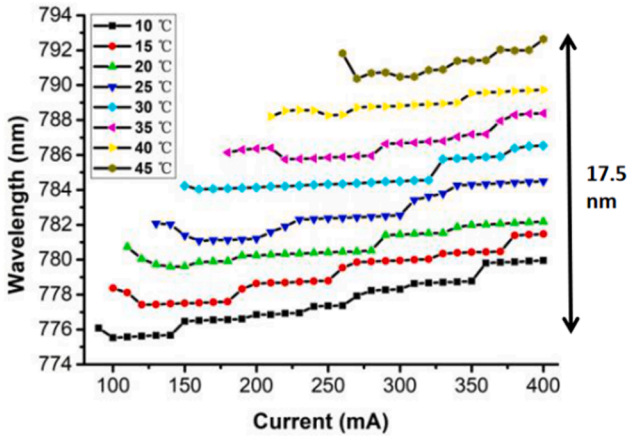

Fig. 5. Center wavelengths of the 780 nm DFB laser diode for different currents and temperatures.

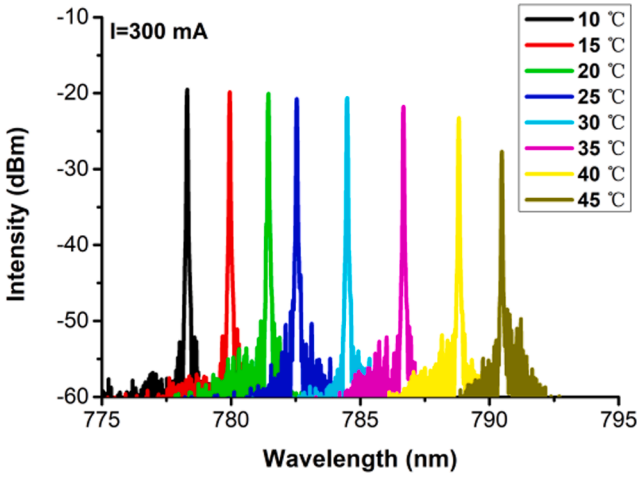

Fig. 6. Center wavelengths of the 780 nm DFB laser diode for different temperatures.,when the injected current is 300 mA.

over 25 dB. The total tuning range of 17.5 nm is much larger than DFB lasers and DBR lasers, under a temperature change of 10–45 °C [17–27].

Fig. 8 demonstrates that the highest SMSR is 36.25 dB at 10 °C when the drive current is 330 mA. The SMSR changes with both temperature

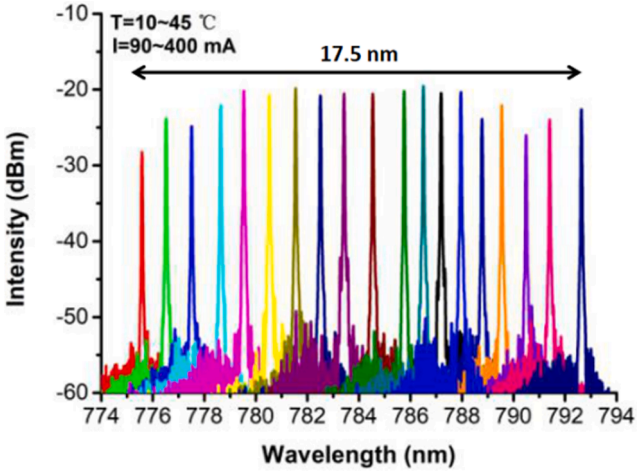

Fig. 7. Spectrum of the 780 nm DFB laser diode for different currents and temperatures.

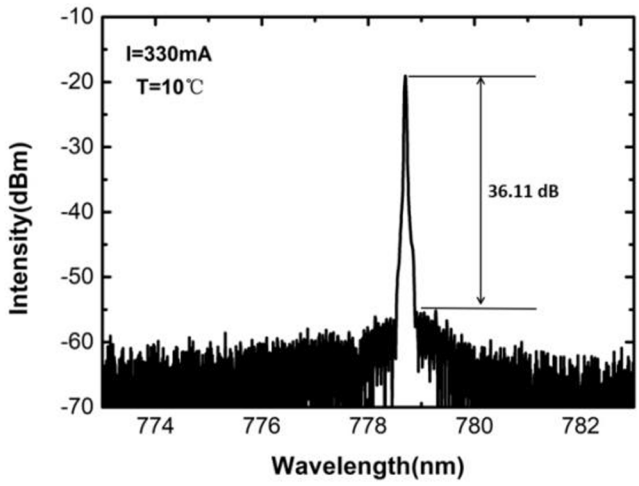

Fig. 8. Center wavelength of the 780-nm DFB laser diode at 10 °C, when the drive current is 330 mA.

and current injection, mainly due to the gain spectrum shift.

Fig. 9 shows the 3 dB linewidth of the device at 20 °C, when the injected current was 300 mA.The linewidth was measured by coupling the collimated laser to the Fabry–Perot interferometer (Thorlabs,

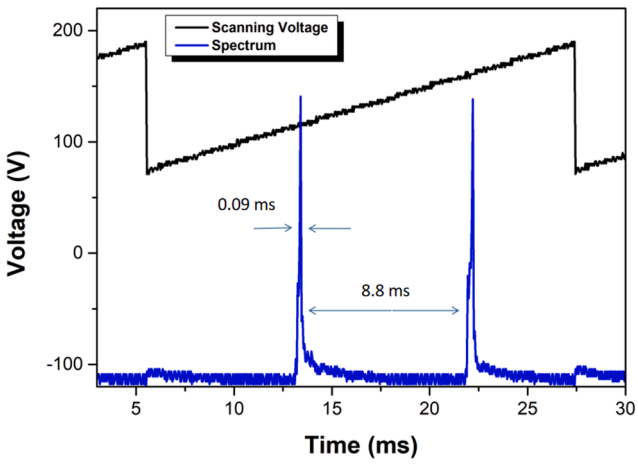

Fig. 9. Linewidth image of the tunable DFB laser working at 300 mA.

SA200-8B), which has a resolution of 67 MHz and free spectral range of 10 GHz. The linewidth is calculated as:$\Delta\nu = (t_{FWHM}/\Delta t) * \nu_0$

where the t_{FWHM} is the full width at half maximum(FWHM) of the scanned spectrum,Δt is the interval between the scanned spectrum, andν_0 is the free spectral range.The 3 dB linewidth was about 100 MHz.

4. Conclusion

We have presented a regrowth-free gain-coupled DFB laser with periodic surface isolation grooves. The device achieves a single longitudinal mode. Our coated device has a SLM CW power of 132.8 mW/facet. Under the help of order hop, a tuning range beyond 17.5 nm can be achieved by controlling the current (through only one pair of electrodes) and the temperature. The maximum SMSR of the device reached 36.25 dB. It provides a novel method for fabricating low-cost, widely tunable 780 nm DFB laser diodes using only i-line lithography without using secondary epitaxy or nano scale lithography. This means that, our technique is suitable for large-scale production which can be applied to many fields such as atomic clocks and gas sensing.

5. Funding sources and acknowledgments

This work is supported by National Science and Technology Major Project of China (2018YFB2200300); Frontier Science Key Program of the President of the Chinese Academy of Sciences (QYZDY-SSW-JSC006); National Natural Science Foundation of China (NSFC) (62090051, 62090052, 62090054, 11874353, 61935009, 61934003, 61904179, 61727822, 61805236, 62004194); Science and Technology Development Project of Jilin Province (20200401069GX, 20200401062GX, 20200501007GX, 20200501008GX, 20200501009GX); Special Scientific Research Project of Academician Innovation Platform in Hainan Province (YSPTZX202034), Dawn Talent Training Program of CIOMP.

Declaration of Competing Interest

The authors declare that they have no known competing financial interests or personal relationships that could have appeared to influence the work reported in this paper.

References

[1] Q. Chen, X. Ma, W. Sun, et al., Demonstration of multi-channel interference widely tunable semiconductor laser, IEEE Photon. Technol. Lett. 28 (24) (2016) 2862–2865.
[2] L.A. Coldren, G.A. Fish, Y. Akulova, et al., Tunable semiconductor lasers: a tutorial, J. Lightwave Technol. 22 (1) (2004) 193–202, 2.
[3] L.A. Coldren, Monolithic tunable diode lasers, IEEE J. Select. Top. Quant. Electron. 6 (6) (2000) 988–999.
[4] R.J. Welty, T.C. Bond, E. Behymer, et al., Integrated laser with low-loss high-index-contrast waveguides for OEICs, Proc. SPIE – Int. Soc. Opt. Eng. 5729 (2005) 49–60.
[5] B. Pan, D. Lu, Y. Sun, et al., Tunable optical microwave generation using self-injection locked monolithic dual-wavelength amplified feedback laser, Opt. Lett. 39 (22) (2014) 6395.
[6] T. Tanabe, S. Ragam, Y. Oyama, Continuous wave terahertz wave spectrometer based on diode laser pumping: potential applications in high resolution spectroscopy, Rev. Sci. Instrum. 80 (11) (2009) 113105.
[7] R. Matthey, C. Affolderbach, G. Mileti, Methods and evaluation of frequency aging in distributed-feedback laser diodes for rubidium atomic clocks, Opt. Lett. 36 (17) (2011) 3311–3313.
[8] J. Vanier, C. Mandache, Appl. Phys. B 87 (2007) 565.
[9] C. Affolderbach, F. Droz, G. Mileti, IEEE Trans. Instrum. Meas. 55 (2006) 429.
[10] V. Ligeret, D. Holleville, S. Perrin, S. Bansropun, M. Lecomte, O. Parillaud, M. Calligaro, M. Krakowski, N. Dimarcq, Electron. Lett. 44 (2008) 804.
[11] D. Budker, M.V. Romalis, Nat. Phys. 3 (2007) 227.
[12] T.L. Gustavson, P. Bouyer, M.A. Kasevich, Phys. Rev.Lett. 78 (1997) 2046.
[13] S. Schilt, A. Kosterev, F. Tittel, Appl. Phys. B 95 (2008) 813.
[14] N. Ueki, A. Sakamoto, Single-transverse-mode 3.4-mW emission of oxide-confined 780-nm VCSELs, IEEE Photon. Technol. Lett. 11 (12) (1999) 1539–1541.
[15] F.M.I. di Sopra, H.-P. Gauggel, M. Brunner, R. Hövel, M. Moser, H.P. Zappe, Electron. Lett. 37 (2001) 832.
[16] G.D. Cole, E. Behymer, T.C. Bond, et al., Short-wavelength MEMS-tunable VCSELs, Opt. Express 16 (20) (2008) 16093–16103.
[17] H. Virtanen, T. Uusitalo, M. Karjalainen, et al., Narrow-linewidth 780-nm DFB lasers fabricated using nanoimprint lithography, IEEE Photonics Technol. Lett. (2017). PP(99):1–1.
[18] F. Gao, L. Qin, Y. Chen, et al., Study of gain-coupled distributed feedback laser based on high order surface gain-coupled gratings, Opt. Commun. 410 (2018) 936–940.
[19] H. Chen, Y. Chen, F. Gao, et al., Narrow-strip 670 nm gain-coupled distributed feedback laser based on periodic anodes fabricated by I-line lithography, IEEE Photon. J. 11 (3) (2019) 1–9.
[20] W.H. Guo, Q. Lu, M. Nawrocka, et al., Nine-channel wavelength tunable single mode laser array based on slots, Opt. Express 21 (8) (2013) 10215.
[21] L.u. Qiaoyin, W.-H. Guo, D. Byrne, J.F. Donegan, Design of slotted single-mode lasers suitable for photonic integration, IEEE Photon. Technol. Lett. 22 (11) (2010) 787–789.
[22] Y. Chen, P. Jia, J. Zhang, et al., Gain-coupled distributed feedback laser based on periodic surface anode canals, Appl. Opt. 54 (30) (2015) 8863.
[23] K. Shima, H. Watanabe, H. Yonetani, et al., Aging characteristics of InGaAsP DFB laser. Optical Fiber Communication Conference, 1988.
[24] J. Fricke, F. Bugge, A. Ginolas, et al., High-power 980-nm broad-area lasers spectrally stabilized by surface Bragg gratings, IEEE Photon. Technol. Lett. 22 (5) (2010) 284–286.
[25] T. Makino, Threshold condition of DFB semiconductor lasers by the local-normal-mode transfer-matrix method: correspondence to the coupled-wave method, J. Lightwave Technol. 12 (12) (1994) 2092–2099.
[26] A.J. Ward, et al., Widely tunable DS-DBR laser with monolithically integrated SOA: design and performance, IEEE J. Select. Top. Quant. Electron. 11 (1) (2005) 149–156, https://doi.org/10.1109/JSTQE.2004.841698.
[27] T. Hirata, M. Suehiro, M. Maeda, et al., Fabrication of 780-nm AlGaAs tunable distributed Bragg reflector laser diodes by using compositional disordering of a quantum well, Jpn. J. Appl. Phys. 30 (Part 1, No. 12A) (1991) 3410–3415.